**The EMBO Journal** Vol. 20 No. 17 pp. 4884–4891, 2001

# Energetic contribution of non-essential 5′ sequence to catalysis in a hepatitis delta virus ribozyme

**I.-hung Shih[1] and Michael D.Been[2]**

Department of Biochemistry, Duke University Medical Center, Durham, NC 27710, USA

[1]Present address: Laboratory of Molecular Biology, National Institute of Diabetes and Digestive and Kidney Diseases, National Institutes of Health, Bethesda, MD 20892, USA

[2]Corresponding author
e-mail: been@biochem.duke.edu

**Hepatitis delta virus (HDV) ribozymes employ multiple catalytic strategies to achieve overall rate enhancement of RNA cleavage. These strategies include general acid–base catalysis by a cytosine side chain and involvement of divalent metal ions. Here we used a *trans*-acting form of the antigenomic ribozyme to examine the contribution of the 5′ sequence in the substrate to HDV ribozyme catalysis. The cleavage rate constants increased for substrates with 5′ sequence alterations that reduced ground-state binding to the ribozyme. Quantitatively, a plot of activation free energy of chemical conversion versus Gibb's free energy of substrate binding revealed a linear relationship with a slope of –1. This relationship is consistent with a model in which components of the substrate immediately 5′ to the cleavage site in the HDV ribozyme–substrate complex destabilize ground-state binding. The intrinsic binding energy derived from the ground-state destabilization could contribute up to 2 kcal/mol toward the total 8.5 kcal/mol reduction in activation free energy for RNA cleavage catalyzed by the HDV ribozyme.**

*Keywords*: catalytic mechanism/catalytic RNA/ground-state destabilization/HDV ribozyme/self-cleaving RNA

## Introduction

Self-cleaving ribozymes encoded in the hepatitis delta virus (HDV) genomic and antigenomic RNA sequences catalyze cleavage of a phosphodiester bond with a rate $10^7$-fold faster than the uncatalyzed reaction (Perrotta and Been, 1991, 1998; Shih and Been, 2001). To account for this significant rate enhancement, several catalytic strategies, including general acid–base catalysis, metal ion catalysis and substrate destabilization, have been proposed for HDV ribozyme-catalyzed RNA cleavage. General acid–base catalysis by a cytosine side chain, C75 in the genomic ribozyme and C76 in the antigenomic ribozyme, is supported by both structural and biochemical data (Ferré-D'Amaré *et al*., 1998; Perrotta *et al*., 1999; Nakano *et al*., 2000; Shih and Been, 2001). An involvement of catalytic divalent metal ions in chemical catalysis is strongly suggested for the HDV ribozymes (Kuo *et al*., 1988; Sharmeen *et al*., 1988; Wu *et al*., 1989; Perrotta and Been, 1990; Suh *et al*., 1993; Shih and Been, 1999; Nakano *et al*., 2000), although there is no structural evidence to support this proposition. For the hammerhead and *Tetrahymena* ribozymes, use of intrinsic binding energy to facilitate catalysis has been demonstrated (Bevilacqua *et al*., 1994; Narlikar *et al*., 1995; Hertel *et al*., 1997; Narlikar and Herschlag, 1998). With the *trans*-acting antigenomic HDV ribozymes, the intriguing observation of an ~25-fold (~2 kcal/mol) difference in dissociation equilibrium constants ($K_d$) between a 10mer substrate and its 3′-cleavage product was consistent with, but not necessarily evidence for, a ground-state destabilization mechanism (Shih and Been, 2000).

Ground-state destabilization is one of the strategies that enzymes employ to maximize the transition-state stabilization. The active site of enzymes may not be geometrically or electrostatically complementary to the substrate at the ground state, but, instead, to the transition-state structure. Specific interactions of an enzyme with the functional groups of the substrates might not be apparent at the ground state, but are revealed at the transition state (Jencks, 1975; Fersht, 1985). Thus, the term intrinsic binding energy refers to the sum of both the ground-state and the transition-state binding energy (Jencks, 1975). Several means by which binding interactions can facilitate chemical conversion include positioning substrates in the active site and thus reducing entropic requirements, desolvating reactive groups on the substrates, and geometrically or electrostatically destabilizing substrates.

Active site components of the HDV ribozymes are proposed to reside in the sequence 3′ to the cleavage site (3′ sequence) because a single nucleoside 5′ to the cleavage site (–1 nucleoside) is sufficient for activity (Perrotta and Been, 1990, 1992). A crystal structure of the genomic 3′ self-cleavage product revealed an intricate tertiary fold with a well-defined active site buried deeply in a cleft formed by P1, J4/2 and P3/L3, leaving minimal space in the catalytic pocket to position the scissile phosphodiester bond and the –1 nucleoside (Ferré-D'Amaré *et al*., 1998). Nevertheless, the –1 nucleoside and scissile phosphate are not only key participants in the reaction but also contain metal-chelating groups that could contribute to catalysis by positioning a catalytic divalent metal ion, or by orienting the scissile phosphodiester bond toward the catalytic residues, or both. Additional 5′ flanking sequence is unlikely to participate directly in chemical catalysis, although longer 5′ sequences can interfere with cleavage activity (Perrotta and Been, 1990, 1991; Chadalavada *et al*., 2000).

To better define the contribution of nucleotides 5′ to the cleavage site (5′ sequence) in HDV ribozyme catalysis, a *trans*-acting form of the antigenomic ribozyme (ADC1) and a series of substrates (Figure 1; Table I) were used for systematic analysis of the effect of length and base

$$E + S \underset{k_{-1}}{\overset{k_1}{\rightleftharpoons}} E \cdot S \underset{[k_{-2}]}{\overset{k_2}{\rightleftharpoons}} E \cdot Pr_{5'} \cdot P_{3'} \underset{[k_{-3}]}{\overset{k_3}{\rightleftharpoons}} E \cdot Pr_{3'} + Pr_{5'} \underset{k_{-4}}{\overset{k_4}{\rightleftharpoons}} E + Pr_{5'} + Pr_{3'}$$

$K_{d\,(S)}$ = 58 nM; $2.1 \times 10^7$ M$^{-1}$ min$^{-1}$; 0.91 min$^{-1}$; ≈ 1.4 min$^{-1}$

$K_{d\,(P5')}$ >> 1 μM; ≥ 12 min$^{-1}$

$K_{d\,(P3')}$ = 2.5 nM; 0.0058 min$^{-1}$; $2.3 \times 10^6$ M$^{-1}$ min$^{-1}$

**Scheme 1**

composition of the 5′ sequence. A minimal kinetic mechanism for ADC1 cleavage of a 10mer substrate, established using pre-steady and steady-state kinetics, serves as a framework for the kinetic characterization presented here (Scheme I) (Shih and Been, 2000). The rate-limiting step for multiple turnover is release of the 3′ cleavage product, which is at least $10^3$-fold slower than dissociation of the 5′ product. Under ribozyme saturating conditions, the chemical transformation is the rate-determining step for the pre-steady state at ~1 min$^{-1}$. This rate is 30-fold slower than that determined for the self-cleaving sequence (Perrotta and Been, 1998; Shih and Been, 2000), giving an overall rate enhancement in the intermolecular form of the reaction of ~$10^6$-fold. In this study, thermodynamic and kinetic parameters were determined for substrates that varied in length and base composition. These studies revealed that the 5′ sequence affected both the stability of the enzyme–substrate (E·S) complex and the rate of chemical conversion. The relationship between these two parameters is consistent with a mechanism in which the 5′ sequence contributes to ground-state destabilization and this free energy is recovered in achieving the transition state.

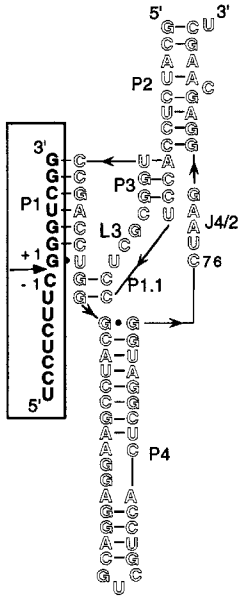


**Fig. 1.** Sequence and secondary structure of the ADC1 ribozyme and a substrate. The *trans*-acting ribozyme and substrate (S15) are shown in outlined and solid letters, respectively. The cleavage site is indicated by an arrow. Paired (P) regions are labeled; J4/2, the sequence joining P4 and P2.

## Results

### *General approaches*

Contributions to HDV ribozyme catalysis by nucleotides 5′ to the cleavage site were examined using the *trans*-acting ribozyme ADC1. ADC1 is derived from the HDV antigenomic ribozyme (Perrotta and Been, 1992) and associates with oligonucleotide substrates through base pairing (Figure 1). ADC1 cleavage of all-RNA substrates follows a kinetic mechanism where the rate constants for substrate dissociation ($k_{-1}$) and the chemistry step ($k_2$) are comparable. Each oligonucleotide substrate used in this study contains the wild-type sequence 3′ to the cleavage site (∧GGGUCGG, where ∧ denotes the cleavage site), but differs in the 5′ sequence (Table I). The naming scheme of substrates (S), deoxynucleotide-containing substrate analogs (DSA) and abasic residue-containing substrate (ABS) includes a number that designates its total length in nucleotides. For the substrates with an abasic residue, a second number is used to designate the position of the abasic site. Kinetic parameters were measured for these substrates using approaches described previously (Shih and Been, 2000). Under ribozyme saturation conditions, the cleavage reactions for all the substrates showed single-exponential kinetics, and active site titration experiments indicated that >90% of the ribozyme was active. In addition, the results from pulse–chase experiments, pH rate profile and kinetic solvent isotope effects are consistent with the chemistry step being rate limiting (Shih and Been, 1999, 2000 and data not shown).

### *Destabilization of the E·Pr$_{3'}$ complex by a 5′ phosphate*

Based on the observation that the $K_d$ for the substrate S10 was ~25-fold higher than that of the 3′ product (Pr$_{3'}$; 5′-GGGUCGG-3′), we had proposed that the scissile phosphodiester linkage at the cleavage site reduced the stability of the E·S complex (Shih and Been, 2000). In the crystal structure of the genomic ribozyme 3′ product (Ferré-D'Amaré *et al*., 1998), the 5′-OH leaving group is within H-bonding distance of the N3 (and O2) of C76. This H-bonding interaction may contribute to the relatively greater stability of the E·Pr$_{3'}$ complex. To assess the destabilizing effect of the scissile phosphodiester linkage on the E·S complex, both $K_d$ and $k_{-1}$ were determined for the 5′-phosphorylated Pr$_{3'}$. Phosphorylation of the 5′-OH leaving group will disrupt H-bond formation between C76 and the 5′-OH group, and partially mimic the scissile phosphodiester at the active site (at pH 8, the monophosphate bears an additional negative charge relative to the phosphodiester). A 4-fold increase in $K_d$ for the 5′-phosphorylated Pr$_{3'}$ (Table II), equivalent to $\Delta\Delta G$ = +0.85 kcal/mol, is consistent with that expected for the loss of one H bond (0.5–2.3 kcal/mol) (Fersht *et al*., 1985; Fersht, 1987; Silverman and Cech, 1999). The lower stability of the E·Pr$_{3'}$-phosphorylated complex was also

**Table I.** Kinetic parameters for single-turnover reactions[a]

| | | $k_2$ ($MgCl_2$) ($min^{-1}$) | $k_2$ ($CaCl_2$) ($min^{-1}$) | $K_M'$ ($MgCl_2$) (nM) | $k_{-1}$ ($MgCl_2$)[b] ($min^{-1}$) | $K_d$ ($MgCl_2$)[c] (nM) |
|---|---|---|---|---|---|---|
| S8 | C∧GGGUCGG | 0.35 | 1.3 | 12 | 0.35 | |
| DSA8 | dC∧GGGUCGG | | | | | 18 |
| S9 | UC∧GGGUCGG | 0.74 | – | 97 | 0.64 | |
| DSA9 | UdC∧GGGUCGG | | | | | 35 |
| S10[d] | UUC∧GGGUCGG | 0.97 | 1.5 | 120 | 1.4 | |
| DSA10 | UUdC∧GGGUCGG | | | | | 58 |
| S12 | UCUUC∧GGGUCGG | 1.0 | – | 143 | 1.6 | |
| DSA12 | UCUUdC∧GGGUCGG | | | | | 65 |
| S15 | UCCUCUUC∧GGGUCGG | 0.43 | – | 225 | 0.86 | |
| DSA15 | UCCUCUUdC∧GGGUCGG | | | | | 50 |
| S8u | U∧GGGUCGG | 0.83 | 0.51 | 33 | 0.64 | |
| DSA8u | dU∧GGGUCGG | | | | | 24 |
| S8a | A∧GGGUCGG | 0.25 | 0.031 | 5.1 | 0.56 | |
| DSA8a | dA∧GGGUCGG | | | | | 10 |
| S8g | G∧GGGUCGG | 0.045 | 0.027 | 300 | <0.2 | |
| DSA8g | dG∧GGGUCGG | | | | | 3.1 |
| ABS9-1 | UX∧GGGUCGG | 0.08 | 0.013 | 40 | 0.78 | – |
| ABS10-1 | UUX∧GGGUCGG | 0.11 | 0.013 | 55 | 1.4 | – |
| ABS10-2 | UXC∧GGGUCGG | 1.8 | 2.7 | 145 | 2.1 | – |

S, all-ribonucleotide substrates; DSA, deoxynucleotide-containing substrate analogs; ABS, abasic residue-containing substrate. –, values were not determined; ∧, cleavage site; X, reduced abasic residue. The deviation of each determination was <15%.
[a]The kinetic parameters were determined in 40 mM Tris–HCl pH 8.0, 1 mM EDTA and 11 mM $MgCl_2$ or $CaCl_2$.
[b]The values for $k_{-1}$ were determined using equation 4 (see Materials and methods).
[c]$K_d$ was determined by gel-shift and inhibition competitive assays using non-cleavable deoxy substrate analogs under the same conditions.
[d]S10 was renamed from S3 (Shih and Been, 2000) for consistency of naming oligonucleotides in this paper.

reflected in its dissociation rate constant ($k_{-1}$), which was 10-fold faster than dissociation of the E·$Pr_{3'}$ complex (data not shown). However, the effect of adding the terminal phosphate group was less than the total difference observed in $K_d$ between E·S and E·$Pr_{3'}$, suggesting that the presence of moieties 5′ to the cleavage site phosphate must also interfere with the stability of the E·S complex.

### *Base specificity at the –1 position*

The effect of varying the base at the –1 position (–1 base) was examined using the oligonucleotide substrate S8 and its –1 variants (S8a, S8g and S8u; see Table I). ADC1 cleaves substrates with any of the four natural bases at the –1 position, but with different efficiencies (Perrotta and Been, 1992). Here, the pre-steady-state parameters were determined for the four substrates. The cleavage rate in 11 mM $MgCl_2$ for these substrates decreased in the following order: U > C > A > G, with the first-order rate constant ($k_2$) for S8u 18-fold higher than that for S8g (Table I). The cleavage rates were relatively faster for pyrimidines than purines at position –1, and this pyrimidine preference was more prominent in $CaCl_2$ than in $MgCl_2$ (Table I). The equilibrium dissociation constants of the four substrates, determined using non-cleavable analogs, varied over an 8-fold range (Table I), suggesting that identity of the –1 base also affected the stability of the E·S complex.

Contributions of the –1 base in cleavage reactions of the HDV ribozyme were further characterized using substrates containing an abasic residue at the –1 position connected through a normal 3′,5′-linked ribose–phosphodiester bond at the cleavage site (–1 abasic substrates). The two –1 abasic substrates ABS9-1 and ABS10-1 shared the remainder of the sequence with the normal substrates S9 and S10 (Table I). The ADC1 ribozyme cleaved the –1 abasic substrates at the correct position, between G+1 and the –1 abasic residue (Figure 2). The 3′ cleavage product generated from ABS9-1 and ABS10-1 co-migrated with that generated from S9 and S10, suggesting that cleavage of the –1 abasic substrates also yielded a 5′-OH group on the 3′ cleavage product. As a control for aberrant cleavage at abasic sites, a substrate containing a single abasic residue at the –2 position, ABS10-2, was also tested with ADC1. ABS10-2 was cleaved at the normal position, generating a 3′ product that migrates with the correct size and bears a 5′-OH group (Figure 2). With each of the three abasic substrates, there was no evidence for enhanced cleavage at other sites.

Although the abasic residue at the –1 position did not affect cleavage-site selection, the kinetics of the cleavage reaction were altered. The first-order rate constants ($k_2$) of the –1 abasic substrates were ~10-fold lower than their corresponding wild-type substrates (Table I). However, moving the abasic residue to the –2 position resulted in a 2-fold increase in $k_2$ relative to the wild-type substrate. For both of the –1 abasic substrates, the substrate dissociation rate constants ($k_{-1}$) were the same as the normal substrates. Thus, $k_{-1}$ was ~10-fold faster than the chemistry step, and cleavage of the –1 abasic substrates followed a Michaelis–Menten mechanism. With both of the –1 abasic substrates, $K_d$ measured by gel-shift assays using an inactive ribozyme, ADC1(76u), was comparable to that of the deoxy substrate analogs (Table II). These numbers were also in good agreement with $K_M'$, as expected for the Michaelis–Menten cleavage mechanism ($K_d = K_M'$). The results suggested that the slower cleavage rate for the abasic substrates was not due to a difference in stability of the E·S complex.

**Table II.** Equilibrium dissociation constants ($K_d$)[a]

| | ADC1(wt) (nM) | ADC1(C76u) (nM) |
|---|---|---|
| ABS9-1 | – | 62 |
| ABS10-1 | – | 87 |
| ABS10-2 | – | 52 |
| DSA9 | 35 | 57 |
| DSA10 | 60 | 89 |
| $Pr_{3'}$[b] | 1.9 | – |
| Phosphorylated-$Pr_{3'}$ | 7.4 | – |

[a]The equilibrium dissociation constants were determined by gel-shift assays in 40 mM Tris–HCl pH 8.0, 1 mM EDTA and 11 mM $MgCl_2$. The deviation between individual determination is within 20%.
[b]$Pr_{3'}$ were renamed from DP3 (Shih and Been, 2000).

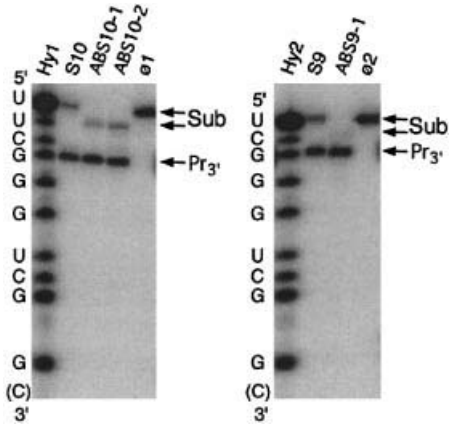


**Fig. 2.** *Trans*-cleavage of abasic and normal substrates by ADC1. The cleavage reactions contained a trace amount of the 3′-end $^{32}$P-labeled oligonucleotide substrate and 1 μM ADC1, in 40 mM Tris–HCl pH 8.0, 1 mM EDTA and 11 mM $MgCl_2$. Reaction times for each substrate were: S10, 1 min; ABS10-1, 30 min; ABS10-2, 1 min; S9, 1 min; ABS9-1, 30 min. Reactions were fractionated on a 20% polyacrylamide gel. The substrate (Sub) and 3′ cleavage product ($Pr_{3'}$) were 3′-end labeled. Hy1 and Hy2 were the alkaline partial digests of S10 and S9, respectively. ø1 and ø2 were untreated substrate S10 and S9, respectively.

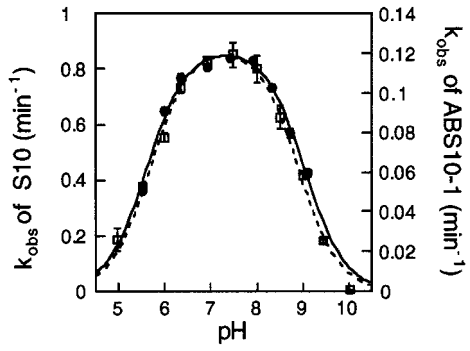


**Fig. 3.** pH dependence of the S10 and ABS10-1 cleavage reactions. The pH profiles of S10 (open squares; dashed line) and ABS10-1 (closed circles; solid line) were performed under $k_{cat}$ conditions with a saturating ribozyme concentration and fit to: $k_{obs} = k_2/(1 + 10^{pK_{a1} - pH} + 10^{pH - pK_{a2}})$. The two apparent p$K_a$ values are 5.7 ± 0.1 and 8.9 ± 0.1 for S10, and 5.6 ± 0.1 and 9.0 ± 0.1 for ABS10-1, respectively.

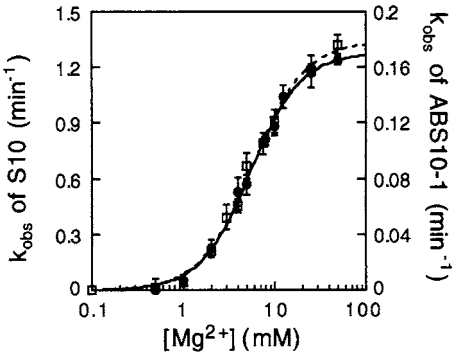


**Fig. 4.** Metal ion concentration dependence of S10 and ABS10-1 cleavage reactions. The first-order rate constants $k_2$ were determined under $k_{cat}$ conditions with a saturating ribozyme concentration at pH 8.0 and varied $MgCl_2$ concentration for S10 (open squares; dashed line) and ABS10-1 (closed circles; solid line). The data were fit to the Hill equation, and the apparent binding constants and Hill constants were 15 and 1.6 mM, respectively, for both S10 and ABS10-1.

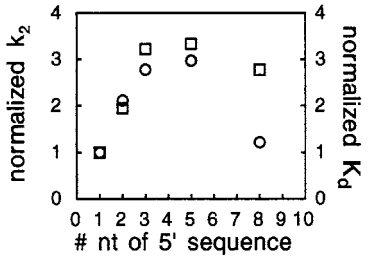


**Fig. 5.** Change in the cleavage rate and dissociation equilibrium constants with increasing length of the 5′ sequence. $k_2$ and $K_d$ were determined for wild-type substrates with length 5′ to the cleavage site varying from 1 to 8 nt (Table I). Both $k_2$ (circles) and $K_d$ (squares) were normalized to those of S8 and plotted against the number of nucleotides in their 5′ sequence.

To examine whether the –1 base interacts with catalytic residues at the active site, the pH dependence of the cleavage reaction was determined with the –1 abasic substrate ABS10-1. ADC1 cleavage of a normal substrate (S10) demonstrated a bell-shaped pH profile (Shih and Been, 1999), with an apparent p$K_a$ of 5.5 possibly reflecting the p$K_a$ of the cytosine side chain at position 76 (C76). The p$K_a$ of C76 may be shifted toward neutral pH by interactions with active site components (Ferré-D'Amaré *et al.*, 1998). The pH dependence of ABS10-1 cleavage is identical to that of S10 (Figure 3), suggesting that the –1 base is not involved in interactions that result in the p$K_a$ shift of C76.

The $Mg^{2+}$ concentration dependence was determined for cleavage of both the normal (S10) and –1 abasic substrates (ABS10-1) (Figure 4). For both reactions, the Hill constant was 1.6 and the apparent $K_d$ was ~15 mM at pH 8.0. The absence of a change in either the Hill constant or apparent $K_d$ suggests that the base at the –1 position does not directly coordinate a catalytic metal ion.

### *Effect of the length of the 5′ sequence on substrate binding and cleavage*

A series of substrates derived from the wild-type sequence, but varying in length from 1 to 8 nucleotides (nt) 5′ to the

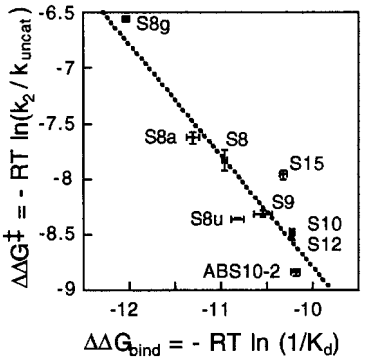


**Fig. 6.** Linear correlation between substrate binding and difference in activation free energy. The Gibb's free energy of substrate binding ($\Delta\Delta G_{bind}$) and activation free energy ($\Delta\Delta G^{\ddagger}$) were calculated as described in the text. The standard errors for both substrate binding and cleavage were plotted, and the substrate used to generate each data point is indicated. The linear correlation of the thermodynamic and kinetic parameters yields a slope of –1.0 ($n$ = 9; $r$ = 0.94).

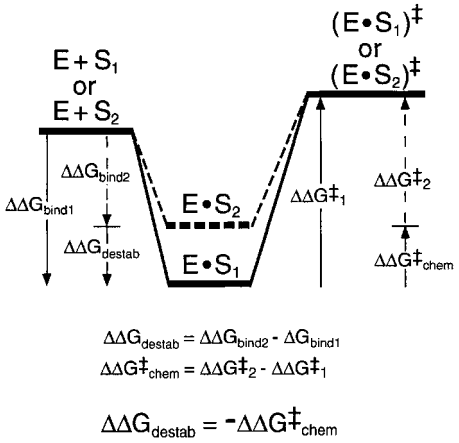


**Fig. 7.** Reaction coordinate diagram of the ADC1 ribozyme cleavage under $k_{cat}$ conditions. Reaction pathways for two substrates, $S_1$ and $S_2$, are shown. The binding energy of substrate $S_2$ is destabilized from that of $S_1$ by $\Delta\Delta G_{destab}$. The activation free energy for $S_2$ cleavage is reduced from that of $S_1$ by $\Delta\Delta G^{\ddagger}_{chem}$. Data for Figure 6 indicated that $\Delta\Delta G_{destab} = -\Delta\Delta G^{\ddagger}_{chem}$. Thus, the reactions of $S_1$ and $S_2$ go through an energetically equivalent transition state.

cleavage site (S8, S9, S10, S12, S15; Table I), were tested in ADC1-catalyzed cleavage reactions. There was a 3-fold increase in $k_2$ as the length of the 5′ sequence increased from 1 to 3 nt, although it appeared to decrease slightly when the 5′ sequence exceeded 5 nt in length (Figure 5, circles). The $K_d$ of these substrates also changed, with a trend similar to that observed for $k_2$ (Table I; Figure 5, squares). Nevertheless, the cleavage reactions of these substrates, which contain the wild-type sequence, followed a similar kinetic mechanism ($k_{-1} \sim k_2$; Table I), and the second-order rate constants ($k_2/K_M'$) did not vary greatly among these substrates, suggesting that the 5′ sequence affected substrate specificity only slightly.

### *Ground-state destabilization*

As shown above, the length and base composition of the 5′ sequence affected both $K_d$ and $k_2$ in a manner qualitatively consistent with a mechanism of ground-state destabilization. From these two parameters, the relative Gibb's free energy for the E·S complex ($\Delta\Delta G_{bind}$) and the difference in activation free energy between HDV-catalyzed and the uncatalyzed reactions ($\Delta\Delta G^{\ddagger}$) were estimated (equations 5.1 and 5.2). With the all-ribonucleotide substrates and ABS10-2, the thermodynamic binding energy ($\Delta\Delta G_{bind}$) demonstrated a linear correlation with activation energy ($\Delta\Delta G^{\ddagger}$), giving a slope close to –1 (Table I; Figure 6). This linear dependence suggests a model where the 5′ sequence causes destabilization of the E·S complex, and the unfavorable binding energy contributes to a lower activation energy barrier for chemical catalysis (Figure 7). Of the substrates tested, S15 exhibited the largest deviation from the linear relationship. The source of this discrepancy was not apparent, but it could be due to the formation of a hairpin structure in S15, which would result in a higher observed $K_d$, or it could be due to unproductive binding of S15 with ADC1, which would lead to lower $k_2$.

## Discussion

### *Dissecting substrate-binding energetics*

Energetic analyses of the contributions of the scissile phosphate, –1 nucleoside and 5′ nucleotides to substrate binding revealed unfavorable binding interactions of the 5′ sequence with the ADC1 ribozyme. The destabilizing effect of the scissile phosphodiester bond was estimated by comparing the binding energy of the 3′ product ($Pr_{3'}$) containing a 5′-OH to that of the 5′-phosphorylated $Pr_{3'}$. A 4-fold increase in $K_d$ was observed ($\Delta\Delta G$ = +0.85 kcal/mol) for the oligonucleotide with the 5′-phosphate. This difference would be consistent with the disruption of a H bond, such as that involving the 5′-OH group and C76. It is also likely that, in the electronegative environment of the active site (Ferré-D'Amaré *et al*., 1998), the additional negative charge on the phosphomonoester causes unfavorable interactions. The stabilizing effect of adding a 5′-dangling nucleoside to an RNA duplex can be as high as –0.3 kcal/mol (Freier *et al*., 1985). Thus, if the –1 nucleoside stacked on the end of P1 and there were no destabilizing interactions, adding the –1 nucleoside (S8) should result in ~1.6-fold stronger binding of the substrate relative to the product. However, in the context of the ADC1 ribozyme, the presence of the –1 nucleoside destabilizes the E·S complex. The $K_d$ of S8 is 2.3-fold higher than the 5′-phosphorylated $Pr_{3'}$ and ~10-fold higher than $Pr_{3'}$. Increasing the number of 5′ nucleotides from one to three reduces the stability of the E·S complex by an additional factor of four. The substrate-binding affinity remained unchanged as the 5′ sequence was increased from 3 to 5 nt, but may become slightly tighter when a substrate with a longer 5′ sequence (8 nt) was used. One explanation for a lower apparent $K_d$ of S15 could be an alternative binding mode with the ADC1 ribozyme. In total, a 3 nt 5′ sequence lowers the stability of the E·S complex by ~2 kcal/mol from that of the E·$Pr_{3'}$ complex.

It is worth noting at this point that the overall thermodynamic equilibrium has not been established in the HDV ribozyme cleavage reaction because the 5′ cleavage product dissociates from the ribozyme readily after cleavage ($k_3 \geqslant 12$ min$^{-1}$; Scheme I) and the ternary complex (E·$Pr_{5'}$·$Pr_{3'}$) is not detectable by gel-shift or gel-filtration assays (Shih and Been, 2000). In the case of the hammerhead ribozyme, which catalyzes a similar chemical reaction, the cleavage reaction is exothermic due to

the penalty paid in product formation of the 2′,3′-cyclic phosphate, but the reaction is spontaneous due to a large gain in entropy upon the formation of two cleavage products (Hertel *et al*., 1994). An entropy-driven reaction could also be the case for the HDV ribozyme, despite the strong binding of the 3′ cleavage product, because of the instability of the $E{\cdot}Pr_{5'}{\cdot}Pr_{3'}$ complex.

### *Intrinsic binding energy in HDV ribozyme catalysis*

The use of intrinsic binding energy for catalysis is characteristic of enzyme-catalyzed reactions where interactions between the substrate and the enzyme at positions away from the reactive residues may not manifest as apparent binding affinity in the ground state but are realized in the transition state (Jencks, 1975). Thus, adding a specific substituent to the substrate could increase the rate of chemical catalysis but cause little or no increase, or even a decrease, in apparent binding. This effect has been demonstrated with many protein enzymes (Jencks, 1975), and more recently with ribozymes (Bevilacqua *et al*., 1994; Narlikar *et al*., 1995, 1997; Hertel *et al*., 1997; Narlikar and Herschlag, 1998). A mechanism of substrate destabilization appears also to be used by the HDV ribozymes. Data presented here suggest that 1–3 nt of the 5′ sequence result in unfavorable interactions in the ground state, which reduces the activation free energy barrier and facilitates chemical conversion. Moreover, a slope of –1 in the plot of Gibb's free energy of binding versus difference in activation free energy (Figure 6) indicates that the increase in $\Delta\Delta G_{bind}$, as a result of substrate destabilization, is equal to the reduction in the activation free energy for chemical catalysis ($\Delta\Delta G^{\ddagger}$). Thus, this relationship reveals that the interactions involving the 5′ sequences are utilized almost solely in ground-state destabilization and not in transition-state stabilization (Figure 7). Furthermore, the slope of –1 implies that each substrate adopts an energetically equivalent transition state because the amount of decreased binding energy is exact payment for the increase in the cleavage rate constant (decrease in the activation energy).

Utilization of intrinsic binding energy to facilitate chemical catalysis can be achieved by substrate desolvation, by destabilizing the substrate electrostatically or geometrically, or by positioning the substrate at the active site, thereby reducing the entropic requirement (Jencks, 1975). Substrate destabilization by electrostatic repulsion in the ground state, which is relieved in the transition state by charge redistribution, has been demonstrated in the *Tetrahymena* ribozyme (Narlikar *et al*., 1995). An analogous model of electrostatic destabilization by a protonated cytosine side chain (C76/C75) (Nakano *et al*., 2000) is possible for the HDV ribozymes (Shih and Been, 2000). Although the identity of the base immediately 5′ to the cleavage site is not critical, contacts made by the 5′ sequence may occur through the ribose–phosphate backbone or result from steric clash. From the crystal structure of the HDV genomic ribozyme 3′ cleavage product, it would appear that the active site, located in a cleft where portions of P1, P3–L3 and J4/2 come together (Bravo *et al*., 1996; Rosenstein and Been, 1996; Ferré-D'Amaré *et al*., 1998), has limited space available for the 5′ sequence. A possible exit site for the 5′ sequence is through an opening between L3 and P1. Accommodation of the 5′ sequence would appear to require a change in the direction of the backbone at the cleavage site phosphate (Ferré-D'Amaré *et al*., 1998). A bend in the scissile phosphodiester may destabilize, for example, the bottom base pairs of P1, but result in a configuration of the ribose–phosphate backbone resembling that of the penta-coordinated transition state for in-line nucleophilic attack. Alternatively, the presence of the 5′ sequence might force the catalytic pocket to adopt a conformation that allows the exit of the 5′ sequence without inducing a sharp bend. In that case, a local conformational adjustment of the ribozyme might facilitate chemical catalysis by better positioning the catalytic residues toward the reactive groups of the substrate, but might also reduce stacking interactions between P1 and P1.1, thereby destabilizing ground-state substrate binding. In either scenario, stress on the substrate or local conformational strain on the ribozyme induced by the 5′ sequence may cause geometrical substrate destabilization (Fersht, 1985).

### *Influence of the –1 base on HDV ribozyme catalysis*

Although there is only limited sequence specificity for the nucleoside at the –1 position, the stability of the E·S complex is affected by the identity of the –1 base. The $K_d$ values of all of the 8mer substrates are higher than that of the 3′ product ($Pr_{3'}$), but they vary for different bases at the –1 position. In particular, the substrates with purines at the –1 position bind to the ADC1 ribozyme more tightly than those with pyrimidines, but they cleave more slowly. It is conceivable that a purine nucleoside at the –1 position, by simply orienting differently than a pyrimidine nucleoside, allows the ribose–phosphate backbone to adopt a configuration that forms a more stable ground-state E·S complex, but, as a result, there is slower chemical conversion.

The base preference for the –1 position is more prominent in the presence of $CaCl_2$ than in $MgCl_2$. In $MgCl_2$, the cleavage rate constants ($k_2$) of the substrates with pyrimidine bases at the –1 position are 1.5- to 18-fold faster than that of the purine or abasic substrates, while the cleavage reactions in $CaCl_2$ showed 20- to 100-fold differences. It has already been argued that direct coordination of the –1 base to a catalytic metal ion is unlikely because the concentration dependence of divalent metal ions for the –1 abasic cleavage reaction is identical to that of the wild-type cleavage reaction. However, the influence of different metal ions on the magnitude of base preference leaves open the possibility that a metal ion is interacting with the scissile phosphate or the ribose at the –1 position, and that this interaction is affected indirectly by base identity.

In contrast to the all-ribonucleotide substrates, or ABS10-2, cleavage of the –1 abasic substrates showed a reduced cleavage rate but no change in the binding constant when compared with the substrates with a pyrimidine as the –1 base. Relative to the normal substrates, binding of the –1 abasic substrate at the active site may not correctly position the scissile phosphodiester bond in the transition state, and this difference may, therefore, result in the reduced cleavage rate. It is also possible that the phosphodiester linkage at an abasic site has more degrees of freedom, resulting in a larger entropic

factor and, thus, a larger activation energy in forming the transition state. Therefore, in addition to a role in ground-state destabilization, the –1 base could, by reducing the entropic penalty, contribute to transition-state stabilization.

### Conclusion

Compared with the uncatalyzed reaction, the rate of cleavage of a phosphodiester bond in an oligonucleotide substrate is increased $10^6$-fold by the *trans*-acting form of the HDV ribozyme. Energetic analyses of cleavage of substrates with different 5′ sequences demonstrated utilization of intrinsic binding energy in HDV ribozyme catalysis. The overall rate enhancement is equivalent to an ~8.5 kcal/mol reduction in the activation free energy. Consistent with the idea that multiple catalytic strategies are employed by enzyme-catalyzed reactions, general acid–base catalysis and, very possibly, metal ion catalysis is critical to HDV ribozyme cleavage. Here we show that substrate destabilization can account for an ~2 kcal/mol reduction in activation free energy and, thus, also contributes significantly to chemical catalysis in the HDV ribozymes.

## Materials and methods

### Materials

T7 RNA polymerase was purified from an overexpressing clone provided by W.Studier (Brookhaven National Laboratory, Upton, NY). Restriction endonucleases, enzymes, chemicals and reagents were purchased commercially. Plasmid DNA used for *in vitro* transcription was purified by CsCl/ethidium bromide equilibrium centrifugation. All-ribonucleotide substrates (S) or DSA were purchased from Dharmacom Research (Boulder, CO). Substrates containing a reduced ABS (Beigelman *et al*., 1994, 1995; Matulic-Adamic *et al*., 1996) were kindly provided by Ribozyme Pharmaceuticals (Boulder, CO).

### Preparation of RNA

*Trans*-acting ribozymes were prepared by *in vitro* transcription using T7 RNA polymerase with *Hin*dIII-linearized plasmid DNA. RNA was separated on denaturing polyacrylamide gels, and recovered by elution and ethanol precipitation. Aliquots of RNA were heated to 95°C in 40 mM Tris–HCl pH 8.0 and 1 mM EDTA immediately before use. Radioactive end-labeling of oligonucleotides was as described previously (Perrotta and Been, 1992).

### Pre-steady-state kinetics

Pre-steady-state kinetic parameters $k_2$ and $K_M'$ were determined from single-turnover cleavage reactions using excess ribozyme ([R]/[S] $\geqslant$ 5) under 'standard conditions' of 40 mM Tris–HCl pH 8.0, 1 mM EDTA and 11 mM $MgCl_2$ at 37°C. The cleavage reactions were initiated by the addition of $MgCl_2$ to a final concentration of 11 mM. Aliquots were quenched in an equal volume of 0.1 M EDTA and fractionated on poly(ethyleneimine) (PEI) plates in 1 M LiCl. The conversion of substrate to product was quantified using a PhosphorImager (Molecular Dynamics). Time courses of single-turnover reactions were fit to a first-order single exponential: $F_t = F_\infty \times (1 - e^{-k_{obs}t})$, where $F_t = F_\infty$ and are the fractions cleaved at time $t$ and end point, respectively, and $k_{obs}$ is the pseudo-first-order rate constant. The first-order cleavage rate constant at saturating ribozyme concentration ($k_2$) and the concentration at which the cleavage rate is half-maximal ($K_M'$) were obtained from a plot of $k_{obs}$ versus ribozyme concentration, which was fit to a Michaelis–Menten equation:

$$k_{obs} = \frac{k_2[E]_{total}}{(K_M' + [E]_{total})}$$

The dependence of the cleavage reaction on divalent metal ion concentration was determined under ribozyme saturating conditions ($k_{cat}$ conditions) in 40 mM Tris–HCl pH 8.0 and various $MgCl_2$ concentrations. To obtain the pH profile for cleavage activity, the reactions were performed at constant ionic strength under $k_{cat}$ conditions at 37°C in 1 mM EDTA, 11 mM $MgCl_2$ and a buffer system containing 25 mM acetic acid/25 mM MES [2-(*N*-morpholino)ethanesulfonic acid]/50 mM Tris pH 4.0–8.0 or 50 mM MES/25 mM Tris/25 mM AMP (2-amino-2-methyl-1-propanol) pH 7.0–10.0.

### Pulse–chase experiments

The dissociation rate constants ($k_{-1}$) of substrates were measured by pulse–chase experiments under standard conditions. Cleavage of a trace amount of 5′-end $^{32}$P-labeled substrate (<2 nM) with saturating ribozyme was initiated by addition of $MgCl_2$ to a final concentration of 11 mM. At time $t_1$, the chase consisting of excess unlabeled 3′ cleavage product ($Pr_{3'}$, 5′-GGGUCGG-3′) was added to the reaction (final concentration 5 μM). At time $t_2$, aliquots were quenched and fractionated as described above. The dissociation rate constant $k_{-1}$ was calculated using two methods as described previously (Shih and Been, 2000). First, $k_{-1}$ was obtained from the ratio of the extent of cleavage in the chase and control reactions ($[P]_{\infty,\ chase}$ and $[P]_{\infty,\ control}$) using equation 1.

$$([P]_{\infty,\ chase} - [P]_{t_1,\ control})/([P]_{\infty,\ control} - [P]_{t_1,\ control}) = k_2/(k_{-1} + k_2) \quad (1)$$

where $[P]_{t1,\ control}$ is the fraction cleaved at time $t_1$, when the chase is added. In the second method, the first-order rate constant ($k_{obs}$) after addition of the chase is the sum of $k_2$ and $k_{-1}$ (equation 2).

$$k_{obs,\ chase} = k_2 + k_{-1} \quad (2)$$

The values obtained from the two methods agreed within ±20%.

$k_{-1}$ was also determined by following dissociation of the E·S complex directly with a gel-shift assay using a 5′-end $^{32}$P-labeled deoxy substrate analog. The two methods gave similar values for $k_{-1}$.

### Gel-shift and competitive inhibition assays

The equilibrium dissociation constants of oligonucleotides with *trans*-acting ribozymes were determined by gel-shift or competitive inhibition assays using 3′ cleavage products, substrates or substrate analogs with a deoxyribonucleotide at the cleavage site. For gel-shift assays, a trace amount of 5′- or 3′-end $^{32}$P-labeled oligonucleotide was pre-incubated with increasing concentrations of ribozyme under standard conditions for 30 min and fractionated on a non-denaturing gel (Shih and Been, 2000). The binding constant ($K_d$) was obtained from a plot of the fraction of bound substrate ($F_{bound}$) versus ribozyme concentration ([E]) using equation 3:

$$F_{bound} = \frac{1}{(1 + K_d/[E]_{total})} \quad (3)$$

Competitive inhibition assays were used to determine the inhibition constant ($K_i$), which is equivalent to $K_d$. Cleavage reactions were carried out under subsaturating ribozyme concentrations ($k_{cat}/K_m$ conditions) with a trace amount of 5′-end $^{32}$P-labeled S10. The second-order rate constants [$(k_2/K_M')_{obs}$] were measured using increasing concentrations of deoxy substrate analogs, and data were fit to equation 4:

$$(k_2/K_M')_{obs} = \frac{(k_2/K_M')}{(1 + [inhibitor]/K_i)} \quad (4)$$

### Calculations of thermodynamic parameters

The relative Gibb's free energy of the E·S complex ($\Delta\Delta G_{bind}$) and the difference in activation free energy between the ADC1-catalyzed and the uncatalyzed reactions ($\Delta\Delta G^{\ddagger}$) were estimated from the following equations:

$$\Delta\Delta G_{bind} = -RT \times \ln(1/K_d^{E\cdot S}) \quad (5.1)$$

$$\Delta\Delta G^{\ddagger} = -RT \times \ln(k_2/k_{uncat}) \quad (5.2)$$

in which $R$ is the gas constant (1.98 cal $K^{-1}$ $mol^{-1}$), $T$ is the reaction temperature (310 K) and $k_{uncat}$ is the background cleavage rate in the absence of ribozyme ($10^{-6}$ $min^{-1}$) (Shih and Been, 1999).

## Acknowledgements

We thank K.M.Weeks and P.C.Bevilacqua for helpful comments and suggestions for interpreting the S15 data; T.S.Wadkins and A.T.Perrotta

for reading the manuscript; and S.Zinnen, L.Beigelman and others at R.P.I. for the oligonucleotides containing abasic sites. This work was supported by NIH grant GM47233.

## References

Beigelman,L., Karpeisky,A. and Usman,N. (1994) Synthesis of 1-deoxy-D-ribofuranose phosphoramidite and the incorporation of abasic nucleotides in stem–loop II of a hammerhead ribozyme. *Bioorg. Med. Chem. Lett.*, **4**, 1715–1720.

Beigelman,L., Karpeisky,A., Matulic-Adamic,C., Gonzales,C. and Usman,N. (1995) New structural motifs for hammerhead ribozymes. Catalytic activity of abasic nucleotide substituted ribozymes. *Nucleosides Nucleotides*, **14**, 907–910.

Bevilacqua,P.C., Li,Y. and Turner,D.H. (1994) Fluorescence-detected stopped flow with a pyrene labeled substrate reveals that guanosine facilitates docking of the 5′ cleavage site into a high free energy binding mode in the *Tetrahymena* ribozyme. *Biochemistry*, **33**, 11340–11348.

Bravo,C., Lescure,F., Laugâa,P., Fourrey,J.-L. and Favre,A. (1996) Folding of the HDV antigenomic ribozyme pseudoknot structure deduced from long-range photocrosslinks. *Nucleic Acids Res.*, **24**, 1351–1360.

Chadalavada,D.M., Knudsen,S.M., Nakano,S. and Bevilacqua,P.C. (2000) A role for upstream RNA structure in facilitating the catalytic fold of the genomic hepatitis δ virus ribozyme. *J. Mol. Biol.*, **301**, 349–367.

Ferré-D'Amaré,A.R., Zhou,K. and Doudna,J.A. (1998) Crystal structure of a hepatitis δ virus ribozyme. *Nature*, **395**, 567–574.

Fersht,A. (1985) *Enzyme Structure and Mechanism*. W.H. Freeman and Co., New York, NY.

Fersht,A.R. (1987) The hydrogen bond in molecular recognition. *Trends Biol. Sci.*, **12**, 301–304.

Fersht,A.R. *et al.* (1985) Hydrogen bonding and biological specificity analysed by protein engineering. *Nature*, **314**, 235–238.

Freier,S.M., Alkema,D., Sinclair,A., Neilson,T. and Turner,D.H. (1985) Contributions of dangling end stacking and terminal base-pair formation to the stabilities of XGGCCp, XCCGGp, XGGCCYp and XCCGGYp helixes. *Biochemistry*, **24**, 4533–4539.

Hertel,K.J., Herschlag,D. and Uhlenbeck,O.C. (1994) A kinetic and thermodynamic framework for the hammerhead ribozyme reaction. *Biochemistry*, **33**, 3374–3385.

Hertel,K.J., Peracchi,A., Uhlenbeck,O.C. and Herschlag,D. (1997) Use of intrinsic binding energy for catalysis by an RNA enzyme. *Proc. Natl Acad. Sci. USA*, **94**, 8497–8502.

Jencks,W.P. (1975) Binding energy, specificity and enzymic catalysis: the circe effect. *Adv. Enzymol. Relat. Areas Mol. Biol.*, **43**, 219–410.

Kuo,M.Y.-P., Goldberg,J., Coates,L., Mason,W., Gerin,J. and Taylor,J. (1988) Molecular cloning of hepatitis δ virus RNA from an infected woodchuck liver: sequence, structure and applications. *J. Virol.*, **62**, 1855–1861.

Matulic-Adamic,J., Beigelman,L., Portmann,S., Egli,R. and Usman,N. (1996) Synthesis and structure of 1-deoxy-1-phenyl-β-D-ribofuranose and its incorporation into oligonucleotides. *J. Org. Chem.*, **61**, 3909–3911.

Nakano,S.-I., Chadalavada,D.M. and Bevilacqua,P.C. (2000) General acid–base catalysis in the mechanism of a hepatitis δ virus ribozyme. *Science*, **287**, 1493–1497.

Narlikar,G.J. and Herschlag,D. (1998) Direct demonstration of the catalytic role of binding interactions in an enzymatic reaction. *Biochemistry*, **37**, 9902–9911.

Narlikar,G.J., Gopalakrishnan,R.S., McConnell,R.S., Usman,N. and Herschlag,D. (1995) Use of binding energy by an RNA enzyme for catalysis by positioning and substrate destabilization. *Proc. Natl Acad. Sci. USA*, **92**, 3668–3672.

Narlikar,G.J., Khosla,M., Usman,N. and Herschlag,D. (1997) Quantitating tertiary binding energies of 2′ OH groups on the P1 duplex of the *Tetrahymena* ribozyme: intrinsic binding energy in an RNA enzyme. *Biochemistry*, **36**, 2465–2477.

Perrotta,A.T. and Been,M.D. (1990) The self-cleaving domain from the genomic RNA of hepatitis δ virus: sequence requirements and the effects of denaturant. *Nucleic Acids Res.*, **18**, 6821–6827.

Perrotta,A.T. and Been,M.D. (1991) A pseudoknot-like structure required for efficient self-cleavage of hepatitis δ virus RNA. *Nature*, **350**, 434–436.

Perrotta,A.T. and Been,M.D. (1992) Cleavage of oligoribonucleotides by a ribozyme derived from the hepatitis δ virus RNA sequence. *Biochemistry*, **31**, 16–21.

Perrotta,A.T. and Been,M.D. (1998) A toggle duplex in hepatitis δ virus self-cleaving RNA that stabilizes an inactive and a salt-dependent pro-active ribozyme conformation. *J. Mol. Biol.*, **279**, 361–373.

Perrotta,A.T., Shih,I.-h. and Been,M.D. (1999) Imidazole rescue of a cytosine mutation in a self-cleaving ribozyme. *Science*, **286**, 123–126.

Rosenstein,S.R. and Been,M.D. (1996) Hepatitis δ virus ribozymes fold to generate a solvent-inaccessible core with essential nucleotides near the cleavage-site phosphate. *Biochemistry*, **35**, 11403–11413.

Sharmeen,L., Kuo,M.Y.-P., Dinter-Gottlieb,G. and Taylor,J. (1988) Antigenomic RNA of human hepatitis δ virus can undergo self-cleavage. *J. Virol.*, **62**, 2674–2679.

Shih,I.-h. and Been,M.D. (1999) Ribozyme cleavage of a 2′,5′-phosphodiester linkage: mechanism and a restricted divalent metal ion requirement. *RNA*, **5**, 1140–1148.

Shih,I.-h. and Been,M.D. (2000) Kinetic scheme for intermolecular RNA cleavage by a ribozyme derived from hepatitis δ virus RNA. *Biochemistry*, **39**, 9055–9066.

Shih,I.-h. and Been,M.D. (2001) Involvement of a cytosine side chain in proton transfer in the rate-determining step of ribozyme self-cleavage. *Proc. Natl Acad. Sci. USA*, **98**, 1489–1494.

Silverman,S.K. and Cech,T.R. (1999) Energetics and cooperativity of tertiary hydrogen bonds in RNA structure. *Biochemistry*, **38**, 8691–8702.

Suh,Y.-A., Kumar,P.K.R., Taira,K. and Nishikawa,S. (1993) Self-cleavage activity of the genomic HDV ribozyme in the presence of various divalent metal ions. *Nucleic Acids Res.*, **21**, 3277–3280.

Wu,H.-N., Lin,Y.-J., Lin,F.-P., Makino,S., Chang,M.-F. and Lai,M.M.C. (1989) Human hepatitis δ virus RNA subfragments contain an autocleavage activity. *Proc. Natl Acad. Sci. USA*, **86**, 1831–1835.

*Received February 22, 2001; revised July 5, 2001; accepted July 12, 2001*